International Journal of Thermophysics, Vol. 17, No. 6, 1996

Practical Determination of Gas Densities from the Speed of Sound Using Square-Well Potentials

K. A. Gillis[1,2] and M. R. Moldover[1]

Received February 2, 1996

The relationships between the first three density virial coefficients (B, C, and D) and the first four acoustic virial coefficients (β_a, γ_a, δ_a, and ε_a) are rederived and a published error relating D to δ_a is corrected. We observe that even if the nth and higher-density virial coefficients of a hypothetical gas are identically zero, the nth and higher acoustic virial coefficients are not zero; they depend on the temperature derivatives of the 1st through $(n-1)$th density virial coefficients. Thus, two density virial coefficients may suffice for a fit to acoustic data with a cubic pressure dependence. These results are exploited by extending the pressure range of fits to previously published speed-of-sound data without either introducing additional parameters or degrading the fits. We deduce gas densities from fits to speed-of-sound data with acoustic virial coefficients having the temperature dependencies calculated from square-well potentials. The estimated densities differ from independent measurements by a few tenths of a percent in an important range of conditions. These estimates require no p–ρ–T data whatsoever.

KEY WORDS: acoustic virial coefficient; gas densities; equation of state; speed of sound; thermodynamic properties; virial coefficients.

1. INTRODUCTION

As precise and accurate speed-of-sound of data for gases have become more available, the problem of deducing other thermodynamic properties from such data has become more urgent. Here, we consider circumstances that we frequently encountered during NIST's studies of numerous candidate replacement refrigerants [1–3]. We measured the speed of sound

[1] Physical and Chemical Properties Division, Chemical Science and Technology Laboratory, National Institute of Standards and Technology, Gaithersburg, Maryland 20899, U.S.A.
[2] To whom correspondence should be addressed.

0195-928X/96/1100-1305$09.50/0 © 1996 Plenum Publishing Corporation

$u(p, T)$ as a function of the pressure p and the temperature T in the vapor phase of many compounds for which few or no accurate equation-of-state data (i.e., p–ρ–T data) had been published. Typically, the data spanned the temperature and pressure range $0.6 \leqslant T/T_c \leqslant 1.0$ and $0.05 \leqslant p \leqslant 1.0$ MPa, and we also needed to estimate the density of these gases in this range. (Here, T_c is the critical temperature.) To do so, we used the density virial equation of state and we represented the temperature dependencies of the first three density virial coefficients (B, C, and D) by the temperature dependencies calculated from hard-core square-well potentials (HCSWP). In so doing we discovered both an error and an oversight in the literature; both are corrected below.

The HCSWP has three parameters which may be chosen as the volume of the hard core, the depth of the square well, and the width of the square well. To represent adequately the speed-of-sound data, it was necessary to use separate triads of parameters for each of the virial coefficients B, C, and D. Thus, little physical significance can be attached to the exact values of the parameters. Nevertheless, the temperature dependencies of the virial coefficients themselves are satisfactory at low and moderate reduced temperatures (e.g., $0.6 \leqslant T/T_c \leqslant 2.0$). Furthermore, these virial coefficients enable one to estimate the densities of the gases within 0.1% over a range of conditions (up to 1 MPa) of importance in many engineering applications. The estimates do not require any p–ρ–T data whatsoever. At very high temperatures, the HCSWP virial coefficients approach positive constants. This feature is not realistic; however, the limiting behavior occurs at temperatures well above T_c, hence it is never encountered when considering fluids used in two-phase heat transfer applications.

In almost every case that we have studied, the HCSWP equation of state underestimates the density of the gas at the lowest temperatures and highest pressures. We do not know the origin of this systematic error. However, if more accurate estimates of gas densities were required, one could account for this systematic underestimate by making an *ad hoc* correlation using the present data and applying the correlation to future data.

The present approach to obtaining thermodynamic properties from speed-of-sound data contrasts with the rigorous algorithm of Trusler and Zarari [4]. These authors deduced the equation of state of methane in the range $1.45 \leqslant T/T_c \leqslant 1.97$ and $0.4 \leqslant p \leqslant 10$ MPa (indicated as methane II and methane III in Fig. 1). They numerically integrated their very accurate speed-of-sound data spanning the same range. The integration does not assume any specific form for the equation of state; however, it requires initial conditions. For initial conditions, Trusler and Zarari used values of the compression factor $Z = p/(\rho RT)$ and its derivative $(\partial Z/\partial p)_T$ that were

obtained by Pieperbeck et al. [5] from p–ρ–T data at 275 K, i.e., at $T/T_c = 1.45$. When the speed-of-sound data were integrated to $T/T_c = 1.97$, the resulting values of ρ differed from independent measurements by only 0.01 %.

We tested the HCSWP approach with the speed-of-sound data $u(p, T)$ for methane that Trusler and Zarari used. As these authors noted, up to seven terms are required to fit u^2 as a polynomial function of the pressure on isotherms. Thus, it was not surprising that the virial equation could not fit the speed-of-sound data within their uncertainty in the same range ($1.45 \leqslant T/T_c \leqslant 1.97$ and $0.4 \leqslant p \leqslant 10$ MPa), even when a fifth virial coefficient E was included. Also, it was not surprising that the estimates of ρ from the virial equation were comparatively poor. In the worst case, the estimated value of ρ differed by 0.5 % from the accepted value of ρ. When we restricted the pressure range on the lowest isotherm to $0.4 \leqslant p \leqslant 6.8$ MPa, but kept the full pressure range for the higher isotherms, the values of ρ deduced from a fit to the speed-of-sound data differed from independent measurements by less than 0.16 % throughout the range of the fitted data. In this range, the HCSWP approach will be useful for other gases when the accurate p–ρ–T data required for the initial conditions do not exist.

We also considered an even more restricted range, methane II in Fig. 1, that is bounded by $1.45 \leqslant T/T_c \leqslant 1.97$ and $0.4 \leqslant p \leqslant 3$ MPa. Here,

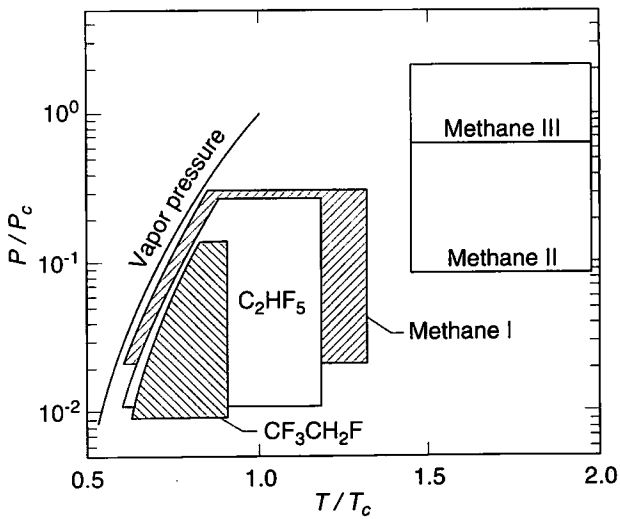

Fig. 1. Location of $u(p, T)$ data sets in reduced temperature and pressure. The vapor-pressure curve is also displayed.

the HCSWP virial equation of state could encompass an additional data set [6] (methane I in Fig. 1) at lower temperatures ($0.66 \leqslant T/T_c \leqslant 1.32$ and $0.02 \leqslant p \leqslant 1.4$ MPa) without either introducing additional parameters or degrading the accuracy of the determination of ρ. Indeed, within this range, the HCSWP densities were within 0.06% of the independently determined densities.

The remainder of this manuscript is organized as follows. First, we review the exact thermodynamic relations connecting the density virial coefficients B, C, D, and E that occur in the expansion of $p(\rho, T)$ to the acoustic pressure virial coefficients β_a, γ_a, δ_a, and ε_a that occur in the expansion of $u^2(p, T)$. Then we introduce the explicit parameters and temperature dependencies resulting from the HCSWP. Finally, we apply the results to several sets of data from the literature.

2. THE VIRIAL EQUATION OF STATE

The equation of state (EOS) of a gas relates the gas pressure p to the temperature T and density ρ (or volume V). For dilute gases, the EOS is often represented as an expansion in $1/V$,

$$pV = RT\left(1 + \frac{B}{V} + \frac{C}{V^2} + \frac{D}{V^3} + \cdots\right) \tag{1}$$

where the virial coefficients B, C, D, etc., are functions of temperature only and R is the universal gas constant. The speed of sound u in a gas may be calculated from the relation

$$u^2 = \left(\frac{\partial p}{\partial \rho}\right)_S = \frac{1}{\rho \beta_S} = \frac{\gamma}{\rho \beta_T} \tag{2}$$

where β_S is the adiabatic compressibility. When Eq. (1) is used for ρ and for β_T in Eq. (2) the result is

$$u^2 = \frac{\gamma RT}{M_m}\left(1 + \frac{2B}{V} + \frac{3C}{V^2} + \frac{4D}{V^3} + \cdots\right) \tag{3}$$

where M_m is the molar mass, $\gamma(T, p)$ is given by

$$\gamma = \frac{C_p}{C_v} = 1 - \frac{T}{C_v}\left(\frac{\partial V}{\partial p}\right)_T \left(\frac{\partial p}{\partial T}\right)_V^2 \tag{4}$$

and the isochoric heat capacity is given by

$$C_V = C_V^o - T\int_V^\infty \left(\frac{\partial^2 p}{\partial T^2}\right)_V dV \tag{5}$$

After substituting Eqs. (1), (4), and (5) into Eq. (3), we have

$$u^2 = \frac{\gamma^o RT}{M_m}\left(1 + \frac{K}{V} + \frac{L}{V^2} + \frac{M}{V^3} + \frac{N}{V^4} + \cdots\right) \tag{6}$$

where γ^o is the ratio of the isobaric to the isochoric specific heats in the limit of zero pressure.

Like the virial equation of state, Eq. (6) is an expansion about the ideal gas limit. The coefficients K, L, M, N, etc., are functions of T only, and they may be expressed in terms of the virial coefficients and γ^o by

$$K = 2B + 2(\gamma^o - 1)\, B_t + \frac{(\gamma^o - 1)^2}{\gamma^o} B_{tt} \tag{7}$$

$$\gamma^o L = (\gamma^o - 1)\, Q^2 + (2\gamma^o + 1)\, C + (\gamma^{o2} - 1)\, C_t + \frac{(\gamma^o - 1)^2}{2} C_{tt} \tag{8}$$

$$\begin{aligned}\gamma^o M = {} & (\gamma^o - 1)^2\, Q^2(2B_t + B_{tt}) + (\gamma^o - 1)\, QP \\ & + 2(\gamma^o + 1)\, D + \frac{2}{3}(\gamma^o - 1)(\gamma^o + 2)\, D_t + \frac{(\gamma^o - 1)^2}{3} D_{tt}\end{aligned} \tag{9}$$

$$\begin{aligned}\gamma^o N = {} & (\gamma^o - 1)^3\, Q^2(2B_t + B_{tt})^2\, B_{tt} + 2(\gamma^o - 1)^2\, Q(2B_t + B_{tt})(C + C_t) \\ & + \frac{(\gamma^o - 1)^2}{2} Q[B + (6\gamma^o - 5)\, B_t + 3(\gamma^o - 1)\, B_{tt}](2C_t + C_{tt}) \\ & + \frac{(\gamma^o - 1)}{4} P^2 + \frac{2(\gamma^o - 1)}{3} Q[3D + (2\gamma^o + 1)\, D_t + (\gamma^o - 1)\, D_{tt}] \\ & + (2\gamma^o + 3)\, E + \frac{(\gamma^o - 1)(\gamma^o + 3)}{2} E_t + \frac{(\gamma^o - 1)^2}{4} E_{tt}\end{aligned} \tag{10}$$

where

$$P = 2C + 2\gamma^o C_t + (\gamma^o - 1)\, C_{tt}$$

$$Q = B + (2\gamma^o - 1)\, B_t + (\gamma^o - 1)\, B_{tt}$$

and we have introduced the notation

$$A_t = T\frac{dA}{dT} \qquad \text{and} \qquad A_{tt} = T^2\frac{d^2A}{dT^2}$$

Usually, the speed of sound is measured as a function of the pressure, not the density. In this case it is more convenient to expand the sound speed in terms of the pressure:

$$u^2 = \frac{\gamma^o RT}{M_m}\left(1 + \frac{\beta_a p}{RT} + \frac{\gamma_a p^2}{RT} + \frac{\delta_a p^3}{RT} + \frac{\varepsilon_a p^4}{RT} + \cdots\right) \tag{11}$$

where the coefficients β_a, γ_a, and ε_a are related to K, L, M, and N by

$$\begin{aligned} \beta_a &= K = RTK' \\ RT\gamma_a &= L - \beta_a B = (RT)^2 L' \\ (RT)^2 \delta_a &= M - \beta_a C - 2RT\gamma_a B = (RT)^3 M' \\ (RT)^3 \varepsilon_a &= N + \beta_a(2BC - D) - B[RT\gamma_a B + 3(RT)^2 \delta_a] - 2LC \end{aligned} \tag{12}$$

[Equation (12) also shows van Dael's [7] definitions of K', L', and M'.]

Equations (7)–(10) and Eq. (12) were derived from Eqs. (1), (2), (4), and (5) with the help of a symbolic mathematics program.[3] The symbolic mathematics program generated the series expansion for the speed of sound, Eq. (6), correct to order ρ^5, from which the coefficients were extracted. The pressure expansion, Eq. (11), was generated from Eq. (6) by iteratively substituting for V from the EOS. The resulting expressions for K and L and the corresponding relations for β_a and γ_a are consistent with the results of van Dael. Likewise, the relation for δ_a is also consistent. However, the expression for M, Eq. (9), disagrees with van Dael's. To our knowledge, the expression for N, Eq. (10), and the corresponding expression for ε_a in Eq. (12) are new results.

Note that the nth acoustic virial coefficient is coupled to the nth density virial coefficient and to all the lower density virial coefficients. For example, the third acoustic virial coefficient γ_a is dependent on B and C, and their temperature derivatives B_t, B_{tt}, C_t, and C_{tt}. There may be a temperature range for which the magnitude of γ_a is mostly dependent on B

[3] The program used was Maple V, Release 2.0b, distributed by Waterloo Maple Software. Brand names and commercial sources of materials, instruments, and software, when noted, are given for scientific completeness. Such information does not constitute a recommendation by the National Institute of Standards and Technology, nor does it suggest that these products are the best for the described purpose.

(and its derivatives) and insensitive to C. If this occurs, a single density virial coefficient B may suffice for a fit to acoustic data with a quadratic pressure dependence. Similar statements apply to δ_a and ε_a. We illustrate this point below with acoustic data for 1, 1, 1, 2-tetrafluoroethane (known as R134a in the refrigeration industry). The acoustic data have a cubic pressure dependence that can be fitted with only two density virial coefficients.

3. THE SQUARE-WELL POTENTIAL

Frequently, the square-well potential is used to correlate equation-of-state and speed-of-sound data for gases. It is particularly convenient because it has only three free parameters and convenient algebraic forms for the density virial coefficients. The temperature dependencies of the second and third virial coefficients for the square-well fluid appear to be consistent with our data over the experimental temperature range, provided that a different set of potential parameters is used for each virial coefficient. The hard-core volumes, well depths, and well widths are adjusted to provide a best fit to the data. Obviously, we are simply exploiting the functional forms provided by the square-well potential and can assign little physical significance to the fitted parameters themselves.

The square-well potential is defined by

$$U(r) = \begin{cases} \infty, & r < \sigma \\ -\varepsilon, & \sigma < r < \lambda\sigma \\ 0, & r > \lambda\sigma \end{cases} \tag{13}$$

for pairwise interactions between particles separated by a distance r. Despite its simplicity, this potential has many features similar to real two-body potentials, namely, a repulsive core, an attractive well, and a finite range. The importance of these characteristics is borne out by further similarities between the calculated properties of the square-well fluid and those of real fluids. On the other hand, the square-well potential has other features that are very different from real potentials, and these differences ultimately impose limitations on this potential as a model of interactions in real fluids. At very high temperatures, $T \gg \varepsilon/k_B$, the square-well fluid behaves like a system of hard spheres instead of a system of compressible spheres. Fortunately, this unrealistic feature is benign since this condition does not occur at temperatures where most gases are chemically stable.

Closed-form expressions for B and C have been calculated from the square-well potential for arbitrary λ. They are

$$B = b_0[1 - (\lambda^3 - 1)\,\Delta] \tag{14}$$

Table I. Values for the Coefficients in Eq. (16) for Three Values of λ

λ	d_0	d_1	d_2	d_3	d_4	d_5	d_6
1.1	0.2869	−0.2207	0.1209	−0.04131	0.006438	-3.090×10^{-4}	-3.023×10^{-6}
1.5	0.2869	−0.1443	−0.1844	−2.920	5.766	−2.197	−0.09867
2.0	0.2869	1.634	−23.29	54.65	70.76	−168.2	−12.74

and

$$C=\frac{b_0^2}{8}(5-c_1\Delta-c_2\Delta^2-c_3\Delta^3)$$

$$\left.\begin{aligned} c_1&=\lambda^6-18\lambda^4+32\lambda^3-15\\ c_2&=2\lambda^6-36\lambda^4+32\lambda^3+18\lambda^2-16\\ c_3&=6\lambda^6-18\lambda^4+18\lambda^2-6 \end{aligned}\right\}\quad \text{for}\quad 1\leqslant\lambda\leqslant 2$$

$$\left.\begin{aligned} c_1&=17\\ c_2&=-32\lambda^3+18\lambda^2+48\\ c_3&=5\lambda^6-32\lambda^3+18\lambda^2+26 \end{aligned}\right\}\quad \text{for}\quad \lambda\geqslant 2 \qquad (15)$$

where $\Delta\equiv e^{\varepsilon/k_BT}-1$.

We were unable to find a published, closed-form expression for the HCSWP fourth virial coefficient D for arbitrary λ. However, expressions for D have been calculated [8] for $\lambda=1.1$, 1.5, and 2.0. These expressions are polynomials in Δ whose coefficients depend on λ:

$$D=b_0^3(d_0+d_1\Delta+d_2\Delta^2+d_3\Delta^3+d_4\Delta^4+d_5\Delta^5+d_6\Delta^6) \qquad (16)$$

Values for the coefficients in Eq. (16) are given in Table I for the three values of λ. We have even less information about the HCSWP fifth virial coefficient E than we do for D. In analogy with the lower virial coefficients, we expect that $E(T)$ can be expressed in the form:

$$E(T)=b_0^4\sum_{i=0}^{10}e_i(\lambda)\,\Delta^i(T) \qquad (17)$$

[The degree of the polynomial for the nth virial coefficient is $n\times(n-1)/2$.] From the hard-sphere virial equation, one knows [9] that $e_0=0.1104$; however, the other coefficients are not known. At high reduced temperatures,

only the lowest terms in Δ are significant. These qualitative considerations led us to test the form

$$E(T) = b_0^4(0.1104 + e_1\Delta(T)) \tag{18}$$

where e_1, b_0, and ε [the latter in the definition of $\Delta(T)$] are treated as adjustable parameters.

4. APPLICATIONS

The utility of HCSWP virial expansion for analyzing $u(p, T)$ data is illustrated with data for three gases. The data used in the following examples span successively wider ranges of reduced temperature and pressure. (See Fig. 1.) Each succeeding example requires additional parameters to fit the pressure dependence of the data. For the first example 6 parameters are used; for the second example, 9 parameters are used; for the third, 11 or 12 parameters are used. Upon attempting to enlarge the range of data in the third example, the practical limit of this method was reached. For each example, we required a representation of the constant-pressure ideal-gas molar heat capacity $C_p^0(T)$. For this purpose, the polynomial

$$C_p^0/R = a_0 + a_1 T + a_2 T^2 + a_3 T^3 + a_4 T^4 \tag{19}$$

was satisfactory.

4.1. 1,1,1,2-Tetrafluoroethane, CF_3CH_2F

The speed of sound $u(p, T)$ was measured by Goodwin and Moldover [10] in 1,1,1,2-tetrafluoroethane (known as R134a in the refrigeration industry). Figure 1 displays the range of reduced temperature and pressure spanned by their data. In the published analysis, the data at the highest pressures on several isotherms were deleted to remove pressure dependence higher than $O(p^2)$. The remaining data were fit with square-well functions for $\beta_a(T)$ and $\gamma_a(T)$. This required the adjustment of six parameters. Three additional parameters [a_0, a_1, and a_2 in Eq. (19)] were used to represent $C_p^0(T)$. When fitting their data, Goodwin and Moldover set $\delta_a(T)$ equal to zero. Their fit of 72 data points using nine adjustable parameters had a reduced χ^2 of 55. The deviations of the data from their fit are shown in Fig. 2.

In fitting their data, Goodwin and Moldover overlooked the substantial contribution to $\delta_a(T)$ from the derivatives of $B(T)$ and $C(T)$. We refit

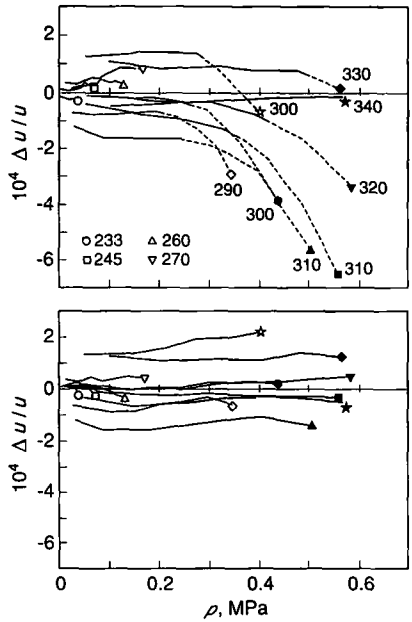

Fig. 2. Deviations of $u(p, T)$ data for CF_3CH_2F from fits of HCSWP virial equation of state. Top: Deviations from the fit of Ref. 10 that omitted $\delta_a(T)$. Bottom: Deviations from present fit using the same functions and the same number of parameters including terms in $\delta_a(T)$ that come from C, C_t, C_{tt}, B, B_t, and B_{tt}. The isotherms are labeled with the kelvin temperature.

their data including this contribution. This contribution to $\delta_a(T)$ permitted us to increase the pressure range of the data without either introducing additional parameters or noticeably degrading the quality of the fit. Figure 2 compares the present fit to the one published by Goodwin and Moldover. The present fit to 94 data points has a reduced χ^2 of 60. The new values of the six parameters used to fit the pressure dependence of these data are tabulated in the Appendix. For completeness, the three parameters used to represent $C_p^0(T)$ are also tabulated in the Appendix.

The deviations from both fits shown in Fig. 2 are dominated by scatter among the zero-pressure intercepts of the isotherms. That is, the pressure dependence of the data has been accounted for leaving deviations for each isotherm that are essentially horizontal lines on the graph. These deviations cannot be removed by either additional parameters or different functions

because the data on experimentally repeated isotherms did not reproduce themselves. (Note the pairs of isotherms at 300 and 310 K.) Goodwin and Moldover [10] attributed this irreproducibility to contamination of the CF_3CH_2F samples from their contact with polymers (electrical insulation, o-rings, etc.) that had been incorporated in their apparatus. (CF_3CH_2F was the first of the alternative refrigerants studied at NIST.) Subsequent measurements of $u(p, T)$ in CF_3CH_2F and other gases (such as C_2HF_5, below) conducted in a polymer-free apparatus did not show deviations of this nature [11].

4.2. Pentafluoroethane, C_2HF_5

The speed of sound in pentafluoroethane (known as R125 in the refrigeration industry) was recently measured by Gillis [2] on isotherms in the temperature and pressure range $0.71 \leqslant T/T_c \leqslant 1.18$ and $0.05 \leqslant p \leqslant 1.00$ MPa. (See Fig. 1.) Boyes and Weber [12] used the Burnett method to

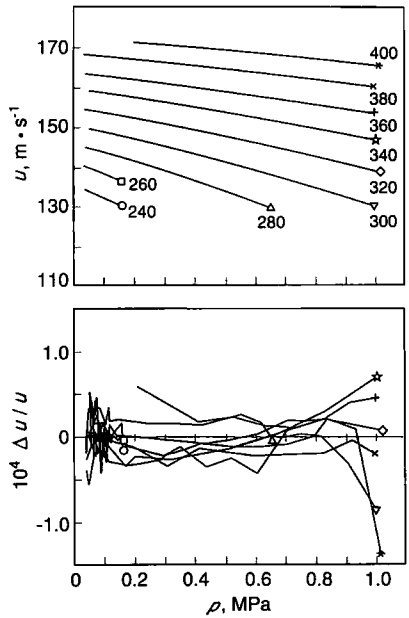

Fig. 3. Top: Measurements of $u(p, T)$ in C_5HF_5 from Ref. 2. Bottom: Deviations of $u(p, T)$ data for C_5HF_5 from fits of HCSWP virial equation of state. The isotherms are labeled with the kelvin temperature.

measure the equation of state of gaseous C_5HF_5 on isochores between 160 and 2800 = mol · m^{-3} in the temperature range $0.80 \leqslant T/T_c \leqslant 1.07$. The pressure extremes were $0.33 \leqslant p \leqslant 4.5$ MPa. Thus these independent sets of data partially overlap and are used here to assess the accuracy of the present method of deducing gas densities from $u(p, T)$.

Figure 3 displays Gillis' fit to the $u(p, T)$ data for C_5HF_5 and the deviations from his fit. Gillis used HCSWP functions for $B(T)$, $C(T)$, and $D(T)$, and he fit the resulting expressions to β_a, γ_a, δ_a, and ε_a. The fit shows random deviations with a fractional root-mean-square deviation of 0.003%. Thus, the HCSWP functions produced a very satisfactory fit to these $u(p, T)$ data. The 12 parameters that Gillis used in this fit are tabulated in the Appendix. Three HCSWP parameters were used to represent each of the three density virial coefficients and three parameters were used to represent $C_p^0(T)$. However, when searching for the "best" values of

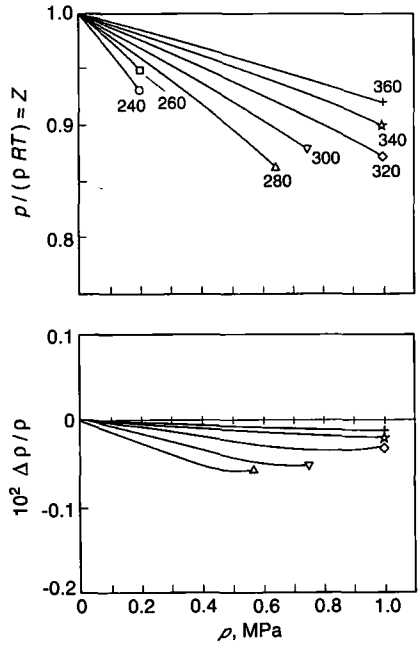

Fig. 4. Top: Compression factor of C_5HF_5 on isotherms where $u(p, T)$ data from Ref. 2 overlap $p\rho T$ data from Ref. 12. Bottom: Fractional deviations of density estimated from $u(p, T)$ data using HCSWP from independent density measurements of Ref. 12.

the 12 parameters, the parameter λ in the definition of $D(T)$ was allowed to assume only three values, 1.1, 1.5, and 2.0, that appear in Table I.

Figure 4 displays the values of Z deduced from the HCSWP for CF_3CH_2F and the deviations of the density $\Delta\rho$ from the values of the density deduced from the Burnett data [12]. The deviations are systematic; the largest deviations are -0.07% and they occur at the highest densities encountered in the $u(p, T)$ data. Density deviations of this size are acceptable for the design of refrigeration machinery because the imperfections in modeling the mechanical components (e.g. the compressor) dominate the uncertainties in the design. The systematic deviations in Fig. 4 are yet another reminder that perfect $u(p, T)$ data are not sufficient to define the equation of state exactly.

4.3. Methane

Recently, very accurate and precise measurements of $u(p, T)$ in methane were made by Trusler and Zarari. For purposes of this discussion, the data are divided into three ranges that are identified in Fig. 1 as methane I, methane II, and methane III. Setzmann and Wagner have published [13] an accurate equation of state based on their comprehensive review of thermodynamic data for methane. Taken together, the work of Trusler and Zarari and that of Setzmann and Wagner contain the information needed to assess the accuracy of the present method of deducing gas densities from accurate $u(p, T)$ data at gas densities that are higher than those encountered in data from our own laboratory.

We attempted to fit the $u(p, T)$ data for methane in three ranges and the results for each range are discussed below. For each range the HCSWP functions for β_a, γ_a, δ_a, and ε_a were used. To extend the fit to higher densities, an additional contribution to $\varepsilon_a(T)$ was used. This contribution was obtained from Eq. (18).

Setzmann and Wagner [13] used spectroscopic information to represent $C_p^0(T)$ for methane as a sum of Einstein functions. For our convenience, we fit their sum by Eq. (19). The resulting five parameters appear in the Appendix even though they were not deduced from the acoustic data.

4.3.1. Methane I + Methane II: $0.66 \leqslant T/T_c \leqslant 1.97$ and $0.05 \leqslant p \leqslant 3.0$ MPa

Figure 5 displays the $u(p, T)$ data for the ranges methane I and methane II in Fig. 1, as well as the deviations from our fit to this data. In the initial attempts to fit these data with the HCSWP functions, the parameter Δ in the expression for $E(T)$ became quite small, indicating that Eq. (18) was approaching its high-temperature limit:

$$E(T) = e'_0 + e'_1/T \tag{20}$$

As an expedient, we adopted the *ad hoc* expression Eq. (20) because HCSWP expressions for $E(T)$ are not available. The parameters that best fit the data are $e'_0 = -3.756 \times 10^{-16}\ \mathrm{m^{12} \cdot mol^{-4}}$ and $e'_1 = 1.092 \times 10^{-13}\ \mathrm{K \cdot m^{12} \cdot mol^{-4}}$ in Eq. (20) and the nine HCSWP parameters tabulated in the Appendix. We remark that Eq. (20) with these values for the parameters cannot be considered a satisfactory HCSWP function because the result $e'_0 < 0$ would imply a core volume that is less than zero.

The deviations from the fit (see Fig. 5) show that nearly all the pressure dependence of the data has been accounted for in the fitting functions. The most conspicuous deviations in Fig. 5 are the scatter among the zero-pressure intercepts of the isotherms. This feature occurred in the deviations for CF_3CH_2F. In effect, the methane data are not consistent with the function used to represent $C_p^0(T)$. However, for methane, the authors [4] attributed this phenomenon to hysteresis in the radius of the acoustic resonator that they used to acquire the data rather than to uncontrolled impurities.

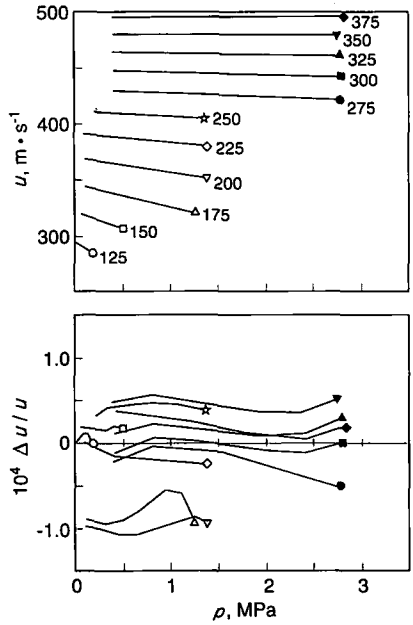

Fig. 5. Top: Measurements of $u(p, T)$ in methane from Refs. 4 and 6 at pressures below 3 MPa. Bottom: Deviations of $u(p, T)$ data from the HCSWP fit.

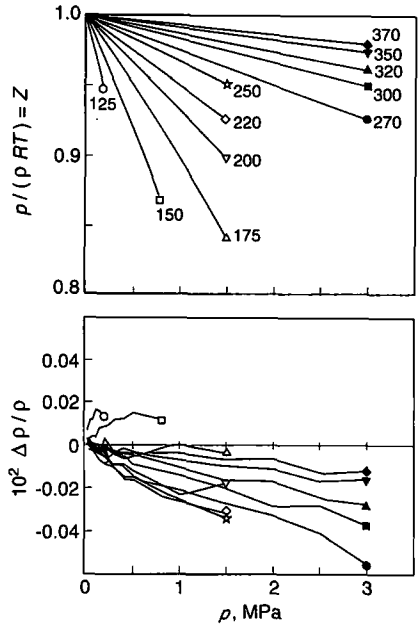

Fig. 6. Top: Compression factor along isotherms of methane. Bottom: Fractional deviations of density estimated from $u(p, T)$ data using HCSWP from the densities tabulated in Ref. 13.

Figure 6 displays the values of Z deduced from the HCSWP for methane and the fractional density deviations $\Delta\rho/\rho$ from the values of the density tabulated in ref. 13. The deviations are systematic and the largest deviation occurs at the highest density; it is only 0.06%, coincidentally about the same as the deviations for C_5HF_5. Thus, in this higher-pressure, higher-temperature range, the HCSWP leads to very satisfactory densities.

4.3.2. Methane II: $1.45 \leqslant T/T_c \leqslant 1.97$ and $0.05 \leqslant p/MPa \leqslant 3.0$

The results for this range were mentioned in Section 1. In this smaller range, the deviations of the $u(p, T)$ data from the fit were a factor of 10 smaller than the deviations shown in Fig. 5. In large part, the better fit is possible because these higher temperature data are more nearly consistent with spectroscopy-based polynomial representation of $C_p^0(T)$. Despite the greatly increased precision of the fit of the $u(p, T)$ data, the densities deduced from the HCSWP functions are essentially identical to those displayed in Fig. 6; thus, they need not be reproduced here. We emphasize

that the densities were deduced solely from acoustic data; they did not any require p–ρ–T data whatsoever.

4.3.3. Methane II + Methane III: $1.45 \leqslant T/T_c \leqslant 1.97$ and $0.05 \leqslant p \leqslant 10$ MPa

As discussed in Section 1, this is the range for which Trusler and Zarari integrated their $u(p, T)$ data. Because of the very high precision of these data, we used Trusler and Zarari's values of $C_p^0(T)$ even though they differ from the spectroscopic values.

The HCSWP functions for $B(T)$, $C(T)$, and $D(T)$ augmented by Eq. (18) for $E(T)$ are unable to fit these $u(p, T)$ data within their accuracy. The fit deviates from the data by as much as 0.06% in $u(p, T)$. The HCSWP functions underestimate the density by as much as 0.75%. This worst case occurs at 10 MPa and 275 K, where the density reaches its highest value, approximately $0.55 \times \rho_c$.

When we restricted the pressure range on the 275 K isotherm to $0.4 \leqslant p \leqslant 6.8$ MPa, the remaining speed-of-sound data were fit within a few

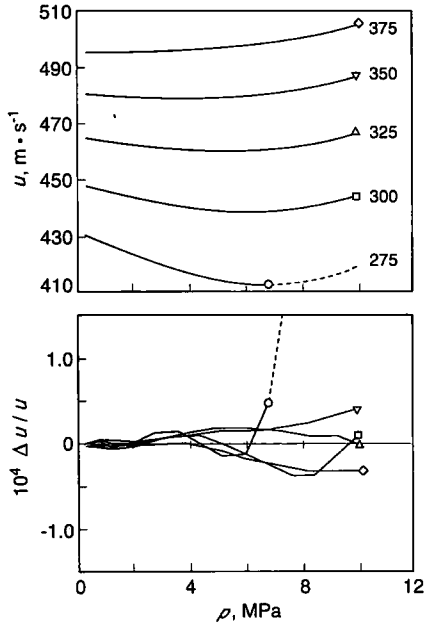

Fig. 7. Top: Measurements of $u(p, T)$ in methane from Refs. 4 and 6 at pressures below 10 MPa. Bottom: Deviations of $u(p, T)$ data from HCSWP fit.

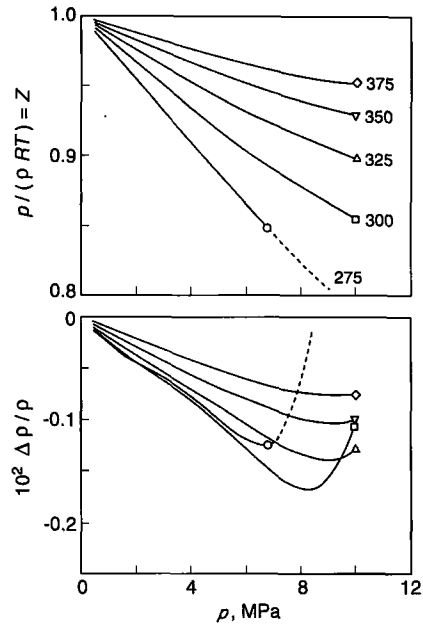

Fig. 8. Top: Compression factor along isotherms of methane. Bottom: Fractional deviations of density estimated from $u(p, T)$ data using HCSWP from the densities tabulated in Ref. 13.

parts in 10^5 by the HCSWP functions for $B(T)$, $C(T)$, and $D(T)$ augmented by Eq. (18) for $E(T)$ (see Fig. 7). The best-fit parameters were $b_0 = 63.992\ \mathrm{cm^3 \cdot mol^{-1}}$, $e_1 = -0.03302$, and $\varepsilon = 1097.15$ K. Figure 8 shows the values of Z that were obtained from the fit by the virial equation of state including E. The resulting values of p differed from independent measurements by less than 0.16% throughout the range $1.45 \leqslant T/T_c \leqslant 1.97$ and $0.4 \leqslant p \leqslant 6.8$ MPa for the lowest isotherm and the range $0.4 \leqslant p \leqslant 10$ MPa on the higher-temperature isotherms.

The dashed curves in Figs. 7 and 8 show the data that were deleted from the fit. In the worst case ($T = 275$ K, $p = 10$ MPa), $\Delta u/u = 0.0018$ and $\Delta\rho/\rho = 0.5\%$.

5. CONCLUSIONS

At the time of this writing, our laboratory has acquired $u(p, T)$ data for 15 candidate alternative refrigerants in approximately the same range of

reduced temperature and pressure as the data for C_5HF_5. For five candidate refrigerants (CF_3CH_2F, C_5HF_5, CHF_2CH_3, CHF_2OCHF_2, and $CF_3CH_2CF_3$), we have been able to compare the derived densities with high-quality independent $p(\rho, T)$ data. In every case, the deviations are approximately the same in sign and magnitude as those shown in Fig. 4 for C_5HF_5. The "law" of corresponding states would predict this result. Thus, if it were necessary, the small systematic deviations shown in Fig. 4 could be reduced by invoking an *ad hoc* "correction" deduced, for example, from Fig. 4.

We have shown that accurate values of gas densities can be deduced solely from high-quality $u(p, T)$ data using HCSWP functions together with the virial equation of state. Small systematic errors in ρ do remain. An important advantage of the HCSWP approach is that the virial coefficients have a physically reasonable temperature dependence. Thus, they can be extrapolated without encountering bizarre results. To illustrate this point, Fig. 9 shows the results of extrapolating densities obtained from the $u(p, T)$ data to the vapor pressure p_σ where the largest systematic errors occur [12].

For CF_3CH_2F and C_5HF_5, the baseline in Fig. 9 represents the density of the saturated vapor $\rho_{V\sigma}$ obtained from the modified Benedict–Webb–Rubin

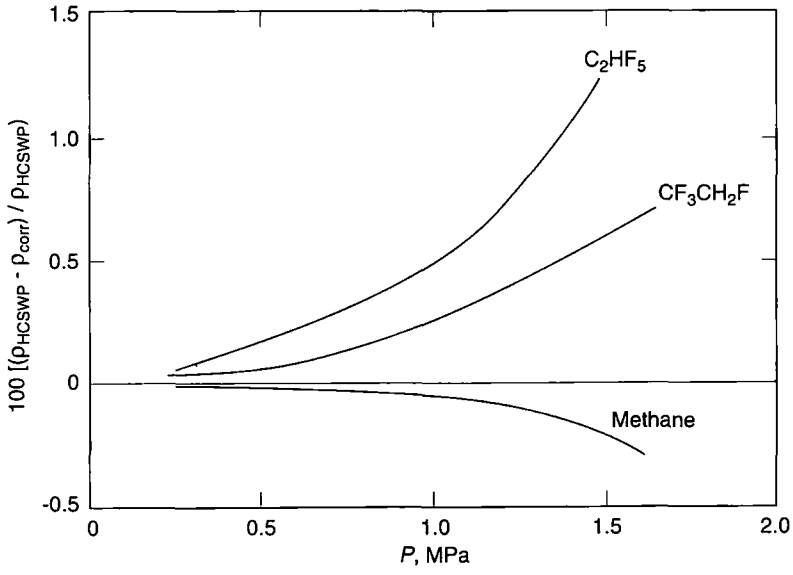

Fig. 9. Comparison of saturated vapor densities $\rho_{V\sigma}$ extrapolated from $u(p, T)$ data using HCSWP functions with $\rho_{V\sigma}$ obtained from multi-parameter multi-property correlations. For CF_3CH_2F and C_5HF_5, the baseline is Ref. 14; for methane, the baseline is Ref. 13.

(mBWR) equations of state provided by the computer package [14] REFPROP 4.0. These mBWR equations were developed by simultaneously fitting many thermodynamic properties over a very wide range of conditions; thus, they are relatively free of large systematic errors; however, they probably do not provide the best possible representations of any specific property such as $\rho_{V\sigma}$ in the range of interest here. For methane, the baseline in Fig. 9 is the Setzmann–Wagner [13] correlation mentioned above.

The $u(p, T)$ data for all three gases were taken on isotherms. For CF_3CH_2F the maximum pressure on each isotherm was the lesser of either 0.6 MPa or $0.6 \times p_\sigma$, for C_2HF_5 the maximum pressure was the lesser of 1.0 MPa or $0.6 \times p_\sigma$, and for methane the maximum pressure was the lesser of 1.0 MPa or $0.8 \times p_\sigma$. Thus, all of the results shown in Fig. 9 are extrapolations. In every case, the extrapolations are well behaved. The "largest" extrapolation (CF_3CH_2F from 0.6 to 1.5 MPa) was a factor of 2.5 in pressure (corresponding to a factor of 3.1 in density). In this case, $\rho_{V\sigma}$ differs from the mBWR $\rho_{V\sigma}$ by 0.7%. In this case, $Z = 0.73$; thus, the extrapolation accounts for almost all of the deviations from ideal-gas behavior. Of course, when a very small extrapolation was required, as was the case for methane, $\rho_{V\sigma}$ is more accurate in the same region. In situations where errors comparable to those shown in Fig. 4 and Figs. 6–9 are acceptable, the vapor-phase equation of state and $\rho_{V\sigma}$ may be determined solely from $u(p, T)$; no vapor-phase p–ρ–T data are required.

APPENDIX

Table AI. Parameters for Hard-Core Square-Well Potentials Used to Fit $u(p, T)$ Data

	B			*C*			*D*		
	b_0 ($cm^3 \cdot mol^{-1}$)	λ	ε (K)	b_0 ($cm^3 \cdot mol^{-1}$)	λ	ε (K)	b_0 ($cm^3 \cdot mol^{-1}$)	λ	ε (K)
CF_3CH_2F	51.615	1.3231	655.6	373.29	1.0907	412.0	0.0		
C_2HF_5	123.01	1.3241	415.63	258.75	1.1151	575.09	105.6	2.0	173.8
CH_4 I&II	48.039	1.6372	131.82	51.987	2.1798	51.189	70.756	2.0	55.98
CH_4 II&III	46.255	1.5784	149.56	51.459	2.0915	50.494	62.669	2.0	95.302

Table AII. Parameters for Ideal-Gas Constant-Pressure Molar Heat Capacity [Eq. (19)]

	a_0	$10^3 a_1$ (K^{-1})	$10^5 a_2$ (K^{-2})	$10^7 a_3$ (K^{-3})	$10^{10} a_4$ (K^{-4})
CF_3CH_2F	2.2540	31.7	−1.68	0.0	0.0
C_2HF_5	3.25482	31.377	−1.42	0.0	0.0
CH_4	3.65821	7.844915	−6.355557	2.074733	−1.964084

REFERENCES

1. K. A. Gillis, *Int. J. Thermophys.* **15**:821 (1994).
2. K. A. Gillis, *Int J. Thermophys.* (in press).
3. A. R. H. Goodwin and M. R. Moldover, *J. Chem. Phys.* **95**:5236 (1991).
4. J. P. M. Trusler and M. P. Zarari, *J. Chem. Thermodynam.* **24**:973 (1992). [Alternative numerical integration schemes requiring p–ρ–T data for initial conditions have been used at pressures much higher than those considered here. See, for example, C. A. ten Seldam and S. N. Biswas, *J. Chem. Phys.* **96**:6163 (1992).
5. N. Pieperbeck, R. Kleinrahm, W. Wagner, and M. Jaeschke, *J. Chem. Thermodynam.* **23**:175 (1991).
6. J. P. M. Trusler and M. Zarari, *J. Chem. Thermodynam.* **27**:771 (1995).
7. W. Van Dael, in *IUPAC Series in Experimental Thermodynamics, Vol.* 2: *Experimental Thermodynamics of Non-reacting Fluids*, B. Le Neindre and B. Vodar, eds. (Butterworths, London, 1975), Chap. 11.
8. E. M. Sevick and P. A. Monson, *J. Chem. Phys.* **94**:3070 (1991).
9. G. C. Maitland, M. Rigby, E. B. Smith and W. A. Wakeham, *Intermolecular Forces: Their Origin and Determination* (Clarendon Press, Oxford, 1981), p. 121.
10. A. R. H. Goodwin and M. R. Moldover, *J. Chem. Phys.* **93**:2741 (1990).
11. K. A. Gillis, M. R. Moldover, and A. R. H. Goodwin, *Rev. Sci. Instrum.* **62**:2213 (1991).
12. S. J. Boyes and L. A. Weber, *J. Chem. Thermodynam.* **27**:163 (1995).
13. U. Setzmann and W. Wagner, *J. Phys. Chem. Ref. Data* **20**:1061 (1991).
14. J. Gallagher, M. McLinden, G. Morrison, and M. Huber, *NIST Thermodynamic Properties of Refrigerants and Refrigerant Mixtures Database, Version* 4.0, NIST Standard Database 23 (National Institute of Standards and Technology, Gaithersburg, MD, 1992).